


Possible Quadrupole Density Wave in the Superconducting Kondo Lattice  $\text{CeRh}_2\text{As}_2$ D. Hafner,<sup>1,\*</sup> P. Khanenko<sup>1</sup>, E.-O. Eljaouhari,<sup>2,3</sup> R. K uchler,<sup>1</sup> J. Banda<sup>1</sup>, N. Bannor,<sup>1</sup> T. L uhmann,<sup>1</sup> J. F. Landaeta<sup>1</sup>, S. Mishra<sup>4</sup>, I. Sheikin<sup>4</sup>, E. Hassinger,<sup>1,5</sup> S. Khim<sup>1</sup>, C. Geibel<sup>1</sup>, G. Zwicky<sup>2</sup>, and M. Brando<sup>1,†</sup><sup>1</sup>Max Planck Institute for Chemical Physics of Solids, 01187 Dresden, Germany<sup>2</sup>Institute for Mathematical Physics, Technische Universit at Braunschweig, 38106 Braunschweig, Germany<sup>3</sup>Universit e de Bordeaux, CNRS, LOMA, UMR 5798, 33400 Talence, France<sup>4</sup>Laboratoire National des Champs Magn etiques Intenses (LNCMI-EMFL), CNRS, Univ. Grenoble Alpes, 38042 Grenoble, France<sup>5</sup>Technical University Munich, Physics Department, 85748 Garching, Germany (Received 13 August 2021; revised 2 November 2021; accepted 16 December 2021; published 3 February 2022)

$\text{CeRh}_2\text{As}_2$  has recently been reported to be a rare case of a multiphase unconventional superconductor close to a quantum critical point (QCP). Here, we present a comprehensive study of its normal-state properties and of the phase (I) below  $T_0 \approx 0.4$  K which preempts superconductivity at  $T_c = 0.26$  K. The second-order phase transition at  $T_0$  presents signatures in specific heat and thermal expansion but none in magnetization and ac susceptibility, indicating a nonmagnetic origin of phase I. In addition, an upturn of the in-plane resistivity at  $T_0$  points to a gap opening at the Fermi level in the basal plane. Thermal expansion indicates a strong-positive-pressure dependence of  $T_0$ ,  $dT_0/dp = 1.5$  K/GPa, in contrast to the strong-negative-pressure coefficient observed for magnetic order in Ce-based Kondo lattices close to a QCP. Similarly, an in-plane magnetic field shifts  $T_0$  to higher temperatures and transforms phase I into another nonmagnetic phase (II) through a first-order phase transition at about 9 T. Using renormalized band-structure calculations, we find that the Kondo effect ( $T_K \approx 30$  K) leads to substantial mixing of the excited crystalline-electric-field states into the ground state. This allows quadrupolar degrees of freedom in the resulting heavy bands at the Fermi level which are prone to nesting. The huge sensitivity of the quadrupole moment on hybridization together with nesting causes an unprecedented case of phase transition into a quadrupole-density-wave state at a temperature  $T_0 \ll T_K$ , which explains the nature of phases I and II.

DOI: [10.1103/PhysRevX.12.011023](https://doi.org/10.1103/PhysRevX.12.011023)Subject Areas: Condensed Matter Physics  
Strongly Correlated Materials  
Superconductivity

## I. INTRODUCTION

Unconventional superconductivity (SC) was first discovered in a heavy-fermion (HF) compound with tetragonal centrosymmetric structure,  $\text{CeCu}_2\text{Si}_2$  [1]. This system, as all other unconventional superconductors, shows single-phase superconductivity at ambient pressure. The only well-established exception to this is  $\text{UPt}_3$  [2–4]. In this material, SC develops within a weak antiferromagnetic

(AFM) order which could be responsible for phase multiplicity [5,6].

A route to realize multiphase SC has been theoretically proposed for spin-singlet quasi-two-dimensional multilayer superconductors in which the combination of Rashba-type spin-orbit coupling and magnetic field leads to two superconducting order parameters separated by a first-order phase transition in field [7]. This scenario seems to be realized in the recently discovered—tetragonal but locally noncentrosymmetric—HF superconductor  $\text{CeRh}_2\text{As}_2$  ( $T_c = 0.26$  K) [8]. Superconductivity emerges from a non-Fermi-liquid (NFL) state, i.e.,  $C/T \propto T^{-0.6}$  and  $\rho(T) \propto \sqrt{T}$ , suggesting proximity to a quantum critical point (QCP) as usually observed in HF systems [9]. Recent As-NQR experiments have detected internal fields at temperatures near  $T_c$ , pointing to an additional AFM order [10]. Moreover, a hump in specific heat at  $T_0 = 0.4$  K, higher than  $T_c$ , was observed, which likely signals some nonidentified order [8]. It is therefore of fundamental

\*daniel.hafner@cpfs.mpg.de

†manuel.brand@cpfs.mpg.de

Published by the American Physical Society under the terms of the Creative Commons Attribution 4.0 International license. Further distribution of this work must maintain attribution to the author(s) and the published article's title, journal citation, and DOI. Open access publication funded by the Max Planck Society.

importance to understand the normal-state properties and to identify possible phases which could compete or coexist with superconductivity in CeRh<sub>2</sub>As<sub>2</sub>.

We report here a comprehensive study of CeRh<sub>2</sub>As<sub>2</sub> based on measurements of the resistivity, specific heat, thermal expansion, magnetostriction, magnetization, and torque done on several single crystals. These are complemented by renormalized-band-structure (RBS) calculations [11–14] using the Dirac-relativistic band-structure code [15]. In the past, these calculations have been proven to agree extremely well with experimental data of strongly correlated electron systems [16–18]. We show that superconductivity is preempted by a nonmagnetic phase (I) evidenced by signatures in specific heat and thermal expansion at  $T_0 \approx 0.4$  K in zero field and by an upturn in resistivity at  $T_0$  suggesting a gap opening at the Fermi level. The analysis of thermal expansion and specific heat data using the Ehrenfest relation results in a strong-positive-pressure dependence of  $T_0$ ,  $dT_0/dp = 1.5$  K/GPa. This is in contradiction with the negative-pressure coefficient expected for magnetic order in Ce-based Kondo lattices close to a magnetic QCP. With  $T_0 = 0.4$  K and  $dT_0/dp = 1.5$  K/GPa,  $T_0$  would be suppressed at a negative pressure of only  $-0.27$  GPa. This result indicates that CeRh<sub>2</sub>As<sub>2</sub> is close to a quantum critical point, but a very unusual one for a Ce-based Kondo lattice since the ordered state occurs on the high-pressure side of the QCP. Similarly, an in-plane magnetic field  $H_{\perp}$  shifts  $T_0$  to higher  $T$ , in contrast to the negative field dependence expected for an antiferromagnetic order. At  $\mu_0 H_{\perp} = 9$  T, we observe a first-order phase transition to a second, nonmagnetic ordered state (phase II) with an even larger positive  $dT_0/dH$ .

Although our experimental techniques cannot directly reveal the order parameter of both phases, our experimental and theoretical results suggest that they are multiorbital in nature despite the tetragonal crystalline electric field (CEF) having a Kramers doublet as the ground state (cf. Supplemental Material [19]). This is surprisingly possible here because the Kondo temperature is very close to the energy of the CEF first excited state, which hybridizes strongly with the ground state allowing quadrupolar degrees of freedom in several heavy bands. Because these bands are also prone to nesting, this situation allows an unprecedented case of “quadrupole-density-wave” (QDW) order, in analogy with the recently proposed “metaorbital” transition [20].

We present first all experimental results and then discuss the possible nature of the new phases I and II. Several normal-state properties of CeRh<sub>2</sub>As<sub>2</sub> have already been presented and discussed in Ref. [8]. Our new results are consistent with those, and the same features are observed in all samples studied here. Information about all samples and batch numbers *B1*, *B2*, and *B3* can be found in the Supplemental Material [19].

## II. RESULTS AND DISCUSSION

A summary of the zero-field data on a sample from *B3* is presented in Fig. 1. The specific heat  $C(T)$  versus  $T$  shows a weak but clear hump starting at  $T_0 = 0.4$  K and a second-order superconducting phase transition at  $T_c = 0.24$  K similar to what was observed in Ref. [8]. Because of the weak signature at  $T_0$ , we employ thermal expansion measurements as another thermodynamic probe to confirm the presence of a phase transition. We measure the thermal expansion coefficients along the  $c$  axis  $\alpha_{\parallel} = 1/l_{\parallel} \times \partial l_{\parallel} / \partial T$  and in the plane  $\alpha_{\perp} = 1/l_{\perp} \times \partial l_{\perp} / \partial T$ .  $\alpha_{\perp}(T)$  is positive in the whole  $T$  range, whereas  $\alpha_{\parallel}(T)$  changes sign near  $T_0$  and  $T_c$ . The volume thermal expansion coefficient  $\beta(T) = \alpha_{\parallel} + 2\alpha_{\perp}$  is, however, overall positive as expected for a Ce-based Kondo-lattice system at  $T < T_K$  [21], where  $T_K$  is the Kondo temperature estimated to be about 30 K for CeRh<sub>2</sub>As<sub>2</sub> [8]. This is because  $\beta(T) = -k_T(\partial S / \partial p)_T$  ( $k_T =$  compressibility), and in Ce-based Kondo-lattice (KL) systems at  $T < T_K$ ,  $\partial S / \partial p$  is negative because increasing pressure enhances  $T_K$ , which results in a decrease of  $S$  at a given  $T$ . On the contrary, below a putative magnetic order at a temperature  $T_m$ ,  $\beta(T)$  is expected to be negative since  $T_m$  decreases with increasing pressure in Ce-based Kondo lattices close to a magnetic QCP [22,23].

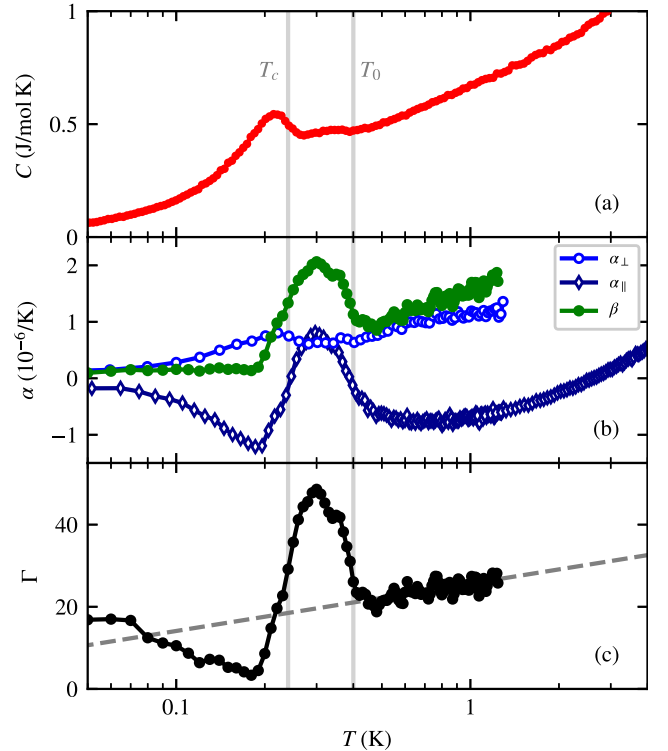


FIG. 1.  $T$  dependence of the (a) specific heat  $C(T)$ , (b) linear and volume thermal expansion coefficients  $\alpha_{\perp}(T)$ ,  $\alpha_{\parallel}(T)$ ,  $\beta(T)$ , and the (c) Grüneisen parameter  $\Gamma(T)$ . The vertical gray lines indicate the onset of the transition at  $T_0$  and  $T_c$ . Measurements done on samples from *B3* ( $l_{\perp} = 2.24$  mm and  $l_{\parallel} = 0.73$  mm).

Both coefficients  $\alpha_{\parallel}(T)$  and  $\alpha_{\perp}(T)$  show steplike anomalies at  $T_c$  as expected for a second-order phase transition. The jump is weak and positive in  $\alpha_{\perp}(T)$  but pronounced and negative in  $\alpha_{\parallel}(T)$ , as sometimes observed in other HF superconductors like CeIrIn<sub>5</sub> [24]. Across  $T_0$ ,  $\alpha_{\parallel}(T)$  exhibits a clear positive increase (approximately equal to  $1.6 \times 10^{-6}/\text{K}$ ), but only a very weak feature is detected in  $\alpha_{\perp}(T)$ . The total jump in  $\beta(T)$  is as large as that at  $T_c$  implying that we also have a second-order phase transition at  $T_0$ . The strong anisotropy in the thermal expansion coefficients is very rare and implies that  $T_0$  is suppressed for a uniaxial stress only along the  $c$  axis. Using the Ehrenfest relation  $dT_c/dp = V_{\text{mol}}T_c(\Delta\beta/\Delta C)$  ( $V_m = \text{molar volume}$ ), we obtain  $dT_c/dp = -0.21 \text{ K/GPa}$  and  $dT_0/dp = 1.5 \text{ K/GPa}$  (see Fig. S5 in the Supplemental Material [19]). So, the pressure dependences have opposite sign, as commonly seen in KL systems close to a QCP at which magnetic order is replaced by a superconducting state. However, in strong contrast to all known Ce-based QCP systems, the  $p$  dependence of  $T_0$  is positive, which implies that the order associated with  $T_0$  is stabilized by pressure, not suppressed as expected and observed for AFM order. With  $T_0 = 0.4 \text{ K}$  and  $dT_0/dp = 1.5 \text{ K/GPa}$ ,  $T_0$  should completely be suppressed at a negative pressure of  $-0.27 \text{ GPa}$ , while  $T_c$  should be slightly enhanced only by about  $57 \text{ mK}$  at this negative pressure. Thus, this analysis based on the Ehrenfest relation indicates that in the  $T_c(p) - T_0(p)$  phase diagram of CeRh<sub>2</sub>As<sub>2</sub> the  $p$  dependence is inverse compared to presently known Ce-based KL superconductors. This reversed  $p$  dependence is a strong indication that the order associated with  $T_0$  cannot be a standard AFM order, in agreement with the lack of signature in ac susceptibility at  $T_0$  (see Ref. [8] and Fig. S4 of the Supplemental Material [19]).

A fundamental quantity in KL systems is the Grüneisen parameter  $\Gamma(T) = k_T V_{\text{mol}} \beta(T) / C(T)$ . The ratio between thermal expansion and specific heat reflects the pressure dependence of the characteristic energy of the system [25]. Since in KL systems close to a QCP the magnetic ordering temperature as well as  $T_K$  are strongly pressure sensitive, their Grüneisen parameter is usually very large and shows a strong  $T$  dependence. This can thus be used as a powerful analyzing tool [25–28].  $\Gamma(T)$  of CeRh<sub>2</sub>As<sub>2</sub> is shown in Fig. 1(c). As expected, it is quite large with a strong and complex  $T$  dependence. The latter property is certainly connected with the two competing orders at  $T_0$  and  $T_c$ . Remarkably,  $\Gamma(T)$  is positive in the whole  $T$  range studied here, as in paramagnetic Ce-based KL systems. This implies that the dominant interaction has a positive  $p$  dependence, suggesting that the dominant interaction that governs the  $p$ -dependent properties of CeRh<sub>2</sub>As<sub>2</sub> might still be the Kondo exchange, i.e., the hybridization between  $4f$  and conduction electrons, as in standard KL systems, but with a different nature of the ordering at  $T_0$ . Thus, combining the analysis of the Grüneisen ratio with the analysis of the Ehrenfest relation indicates that increasing

the  $4f$  hybridization stabilizes the ordering at  $T_0$ . A further notable result is that the  $T$  dependence of  $\Gamma(T)$  above  $T_0$  does not show any evidence for the divergence expected at a QCP. Instead it seems to decrease logarithmically with decreasing  $T$ . Only well below  $T_c$  it seems to increase with decreasing  $T$  reaching values of about 20, sometimes observed in other HF superconductors [21,24]. Since other properties as, e.g., the NFL behavior seen in the specific heat supports the closeness to a QCP, the absence of a well-defined divergence in  $\Gamma(T)$  and its complex  $T$  dependence might be the result of multiple competing phenomena.

We then investigate the effect of an in-plane magnetic field  $H_{\perp}$  on the properties of CeRh<sub>2</sub>As<sub>2</sub> in order to gain more information about the phase associated with  $T_0$ . This is summarized in Fig. 2 in which we plot the resistivity  $\rho(T)$ , the electronic specific heat coefficient  $[C(T) - C_N(T)]/T$ , and the in-plane thermal expansion coefficient  $\alpha_{\perp}(T)$  at different  $\mu_0 H_{\perp}$ . We first analyze  $\rho(T)$  measured on the same sample of Ref. [8] and shown in Fig. 2(a). As explained in Ref. [8], the drop due to SC in  $\rho(T)$  is found at a higher temperature ( $0.39 \text{ K}$ ) than the  $T_c$  detected in specific heat or susceptibility. This is ascribed to inhomogeneity in the material as known from other HF systems [29,30]. This effect prevents us from seeing which feature  $\rho(T)$  may exhibit at  $T_0 = 0.4 \text{ K}$ . Fortunately, since  $T_0$  increases with increasing  $H_{\perp}$  while superconductivity is suppressed at  $\mu_0 H_{c2} \approx 2 \text{ T}$  (cf. Fig. 4), we can detect and follow the signature at  $T_0$  for  $\mu_0 H_{\perp} \geq 2 \text{ T}$ . In Fig. 2(a), the resistivity  $\rho(T)$  measured with  $\mu_0 H_{\perp} = 2 \text{ T}$  shows a clear change in the slope starting at  $T_0 = 0.4 \text{ K}$ . This is confirmed by a plot of the temperature derivative  $d\rho(T)/dT$  vs  $T$  (see Fig. S3 of the Supplemental Material [19]). While  $\rho(T) \propto \sqrt{T}$  above  $T_0$  (see Fig. S2 in Supplemental Material [19]), it shows a slight upturn below  $T_0$ , also visible at higher fields of 3 and 6 T. At 3 T the value of  $\rho(0.1 \text{ K})$  is increased by more than 19% compared to the value extrapolated from  $\rho(T)$  above  $T_0$ . This kind of signature is generally observed at spin-density-wave (SDW) [31] or charge-density-wave (CDW) [32] phase transitions and indicates the opening of a gap at the Fermi level caused by nesting. Since the current is applied in the basal plane of the tetragonal structure, this implies that the propagation vector of the order parameter below  $T_0$  has a component within the basal plane.

The upturn in  $\rho(T)$  disappears for  $\mu_0 H_{\perp} \geq 10 \text{ T}$ , after which we observe a broad crossover from  $\rho(T) \propto \sqrt{T}$  into a Fermi-liquid-like behavior  $\rho(T) \propto T^2$  [see fit on 12 T curve in Fig. 2(a)]. The crossover temperatures coincide with phase-transition temperatures observed in thermal expansion and specific heat (cf. Fig. 4). In contrast, the evolution of the shape of the anomalies in  $\rho(T)$  and  $C(T)/T$  with increasing field differs remarkably. In  $\rho(T)$  the kink at  $T_0$  is most pronounced in the field range  $2 \leq \mu_0 H_{\perp} \leq 8 \text{ T}$ . On the other hand, the small kink

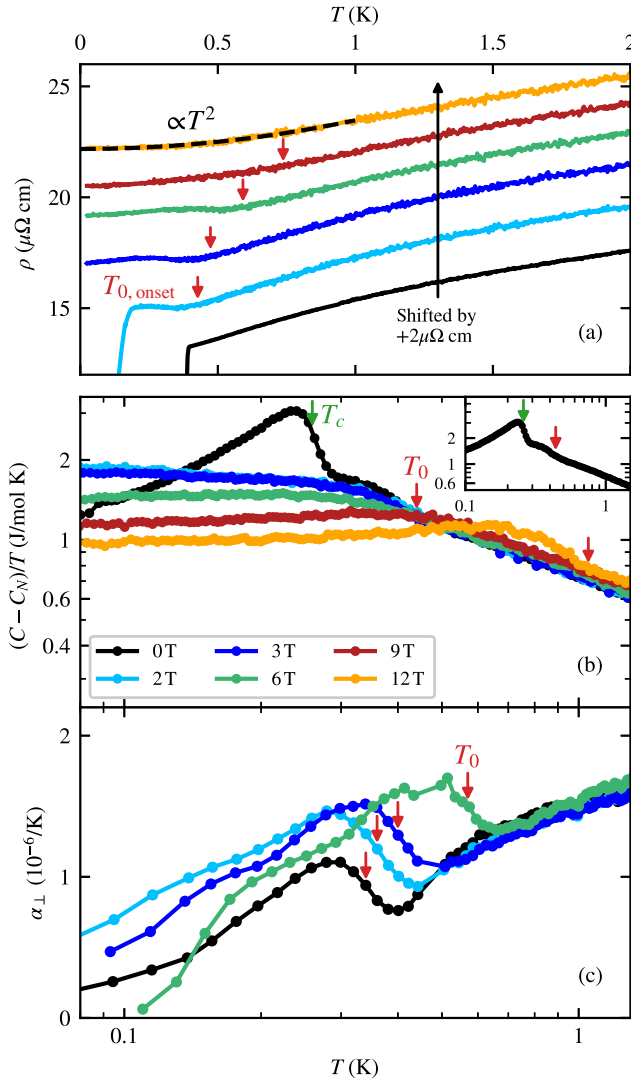


FIG. 2.  $T$  dependence of the (a) resistivity  $\rho(T)$ , (b) electronic specific heat coefficient  $(C - C_N)/T$ , and (c) linear thermal expansion coefficient  $\alpha_{\perp}(T)$ .  $C_N$  is the nuclear contribution to the specific heat. Green and red arrows indicate  $T_c$  and  $T_0$ , respectively. Measurements done on samples from batches B1 and B2 with  $H_{\perp}$  perpendicular to the  $c$  axis.

discernible in  $C(T)/T$  at  $T_0$  in zero field [Fig. 2(b)] becomes weaker with increasing field so that in the range  $3 \leq \mu_0 H_{\perp} \leq 10$  T only a broad hump is visible. But surprisingly, at even higher fields it sharpens again and for  $\mu_0 H_{\perp} \geq 10$  T becomes a well-defined maximum in  $C(T)/T$ . This is corroborated by the behavior of  $\alpha_{\perp}(T)$  in fields  $H_{\perp} \geq H_{c2}$  shown in Fig. 2(c). The steplike increase of  $\alpha_{\perp}(T)$  at  $T_0$  is well pronounced at these fields and increases with increasing field remaining positive for  $H_{\perp} \leq 8$  T. But for  $H_{\perp} > 8$  T, it shows a distinct drop to negative values [see inset of Fig. 3(a)], as it is expected, e.g., for a second-order phase transition from a paramagnetic state into a magnetically ordered phase, like in the SDW phase of  $\text{CeCu}_2\text{Si}_2$  [17]. This behavior is the first

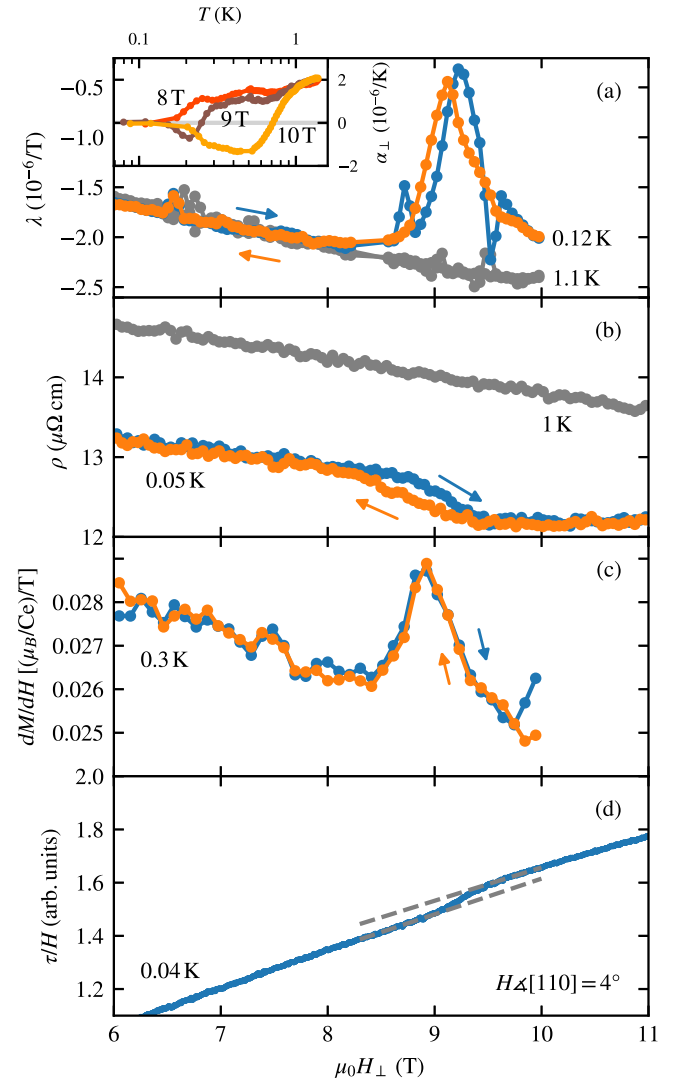


FIG. 3. Field dependence of (a) the magnetostriction coefficient  $\lambda(H)$ , (b) resistivity  $\rho(H)$ , (c) field derivative of magnetization  $dM(H)/dH$ , and (d) torque  $\tau(H)/H$  with field  $H_{\perp}$  applied within the basal plane. The inset of panel (a) shows the  $T$  dependence of the in-plane thermal expansion coefficient  $\alpha_{\perp}(T)$  for fields  $\mu_0 H_{\perp} \geq 8$  T. Measurements done on samples from B2.

indication of a magnetic-field-induced phase transition at a field of about 9 T.

For this reason, we measure the  $H_{\perp}$  dependence of the magnetostriction coefficient  $\lambda(H) = 1/\mu_0 l_0 \times \partial l / \partial H$ , resistivity  $\rho(H)$ , magnetization  $M(H)$ , and torque  $\tau(H) = \mathbf{M} \times \mathbf{H}$ . The results are summarized in Fig. 3. We clearly observe a first-order phase transition at  $\mu_0 H_{\text{cr}} = 9$  T in the form of a large peak in  $\lambda(H)$  ( $\Delta\lambda \approx 2.0 \times 10^{-6}/\text{T}$ ), a drop in  $\rho(H)$ , both with clear hysteresis, and a very small upturn in  $M(H)$  ( $\Delta M \approx 0.003 \mu_B/\text{Ce}$ ) which is better identified in the derivative  $dM(H)/dH$ . All features vanish at  $T \geq 1$  K (gray points). The clear sign change in  $\alpha_{\perp}(T)$  at the transition temperature for  $H_{\perp} \geq H_{\text{cr}}$  [inset of Fig. 3(a)]

and the peak in  $\lambda(H)$  at  $H_{\text{cr}}$  definitively rule out a Lifshitz-like transition [33] or a kind of metamagnetic transition [34,35] and could indicate a transition into a magnetically (purely dipolar) ordered state. However, the very weak features in  $M(H)$ ,  $\tau(H)$ , and  $\rho(H)$  point to a phase transition into another multipolar phase possibly with induced weak dipolar moment. This is corroborated by the lack of features in  $\chi(T)$  for  $H_{\perp} \geq H_{\text{cr}}$  (see Fig. S4 of the Supplemental Material [19]). The field-induced transition is first order as expected when there is a change from one order parameter to another.

We present now the  $T - H_{\perp}$  phase diagram in Fig. 4. It summarizes our experimental results on samples from batches *B1* and *B2*, together with those (superconducting phase SC1) already presented in Ref. [8]. We omit some  $T_0$  points from  $C(T)$  between 5 and 9 T since the transition is too broad to allow us to identify a well-defined transition temperature. In zero field,  $\text{CeRh}_2\text{As}_2$  undergoes a phase transition at  $T_0 \simeq 0.4$  K into a nonmagnetic phase I and then into a superconducting phase SC1 at  $T_c = 0.26$  K. We do not find signatures of any other transition.  $T_0$  increases with an in-plane field  $H_{\perp}$  at a rate of about 0.04 K/T up to the critical field  $\mu_0 H_{\text{cr}} = 9$  T after which it increases much more steeply at about 0.14 K/T. At this critical field, a vertical, first-order phase boundary separates phase I from another phase II whose primary order parameter is also nonmagnetic. Thus, this line corresponds to a sort of “metamultipolar” transition. The point ( $T_{\text{cr}} = 0.7$  K,  $H_{\text{cr}} = 9$  T) at which this vertical phase boundary meets the  $T_0(H)$  boundary corresponds to a tricritical point.

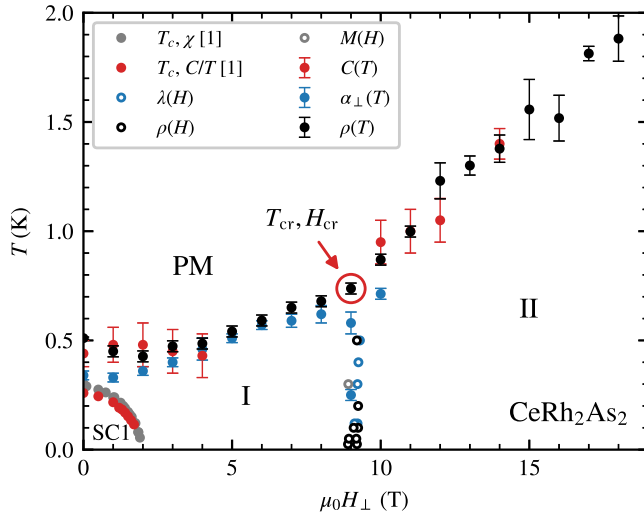


FIG. 4.  $T - H_{\perp}$  phase diagram of  $\text{CeRh}_2\text{As}_2$ . The points on the phase diagram are extracted from measurements performed on samples from *B1* and *B2* which show the same  $T_c$  and  $T_0$ . The point ( $T_{\text{cr}} = 0.7$  K,  $H_{\text{cr}} = 9$  T) is the tricritical point at the end of the first-order boundary which separates phase I from phase II. If error bars are not displayed, they are smaller than the symbols. The points for the SC  $T_c$  were first published in Ref. [8].

We discuss now the possible nature of the two phases I and II and their possible relation to SC. Specific heat and especially thermal expansion data provide clear evidence for the presence of a bulk thermodynamic second-order phase transition at  $T_0$ . In such a Kondo lattice one would usually assume  $T_0$  to indicate AFM order. However, this is in disagreement with several experimental results: no related features in the susceptibility and magnetization (cf. Ref. [8] and Fig. S4 of the Supplemental Material [19]) and the positive pressure and magnetic field dependence of  $T_0$ . The latter property immediately suggests a quadrupolar or a more complex multipolar order. On the other hand, this positive field dependence of  $T_0$  contradicts a valence transition as well as a structural CDW transition, which would anyway be very unlikely at such a low  $T_0$ .

Multipolar ordered states are observed in Ce-based systems with cubic CEF symmetry arising from the quadrupolar degrees of freedom of a quartet ground state as in  $\text{CeB}_6$  [36–38] or  $\text{Ce}_3\text{Pd}_{20}\text{Ge}_6$  [39]. But in  $\text{CeRh}_2\text{As}_2$  the tetragonal CEF splits the  $J = 5/2$  Hund’s rule ground state of  $\text{Ce}^{3+}$  into three Kramers doublets  $|\Gamma(i), \tau\rangle$ ,  $i = 0, 1, 2$ , that have only a spin degree of freedom  $\tau = \pm$ . A determination of the CEF scheme (see Supplemental Material [19]) puts the first and the second excited CEF doublets at  $\Delta_1 \simeq 30$  K and  $\Delta_2 \simeq 180$  K above the CEF ground-state doublet, respectively. Thus, at  $T_0 \simeq 0.4$  K only the CEF ground state is populated, which does not bear a quadrupolar degree of freedom, and therefore, quadrupolar or multipolar order should not be possible.

A quadrupolar order arising unexpectedly from a similar tetragonal CEF was found in  $\text{YbRu}_2\text{Ge}_2$  [40] at  $T_0 = 10.2$  K. In this compound, the small level splitting  $\Delta_1 \simeq 12$  K  $\approx T_0$  allows effective intersite interactions between the multipole moments of the CEF levels to induce a quadrupolar order parameter [41]. In such a case, the ordering temperature can hardly be below  $\Delta_1/2$ . While  $\text{CeRh}_2\text{As}_2$  has a similar  $\Delta_1 \simeq 30$  K,  $T_0 \simeq 0.4$  K is almost 2 orders of magnitude lower than that, making this scenario very unlikely for our case. But, there is another energy scale which plays a fundamental role in  $\text{CeRh}_2\text{As}_2$ : the Kondo temperature  $T_K \approx 30$  K [8], which has been shown to affect the quadrupole moment of CEF-split  $4f$  states [42–45]. As  $\Delta_1 \simeq T_K$ , the formation of the heavy-Fermi-liquid state leads to a significant admixture of excited CEF states to the low-energy states. This is revealed by our RBS calculations whose main results are shown in Fig. 5. Of particular interest is the expectation value of the quadrupole moment  $Q$  which depends on the differences in the population of the Kramers doublets. The influence of the Kondo effect can be seen in Fig. 5(d) in which we compare the variation with temperature  $T$  of  $Q(T) = \sum_{\Gamma(i), \tau} \langle \Gamma(i), \tau | 3J_z^2 - \mathbf{J}^2 | \Gamma(i), \tau \rangle n_{\Gamma(i), \tau}(T)$  for a Ce impurity in a dilute magnetic alloy in the presence of the Kondo effect ( $T_K = 30$  K,  $n_f = 0.9$ , full line) and in the local moment regime ( $T_K = 0$ ,  $n_f = 1$ , dotted line).

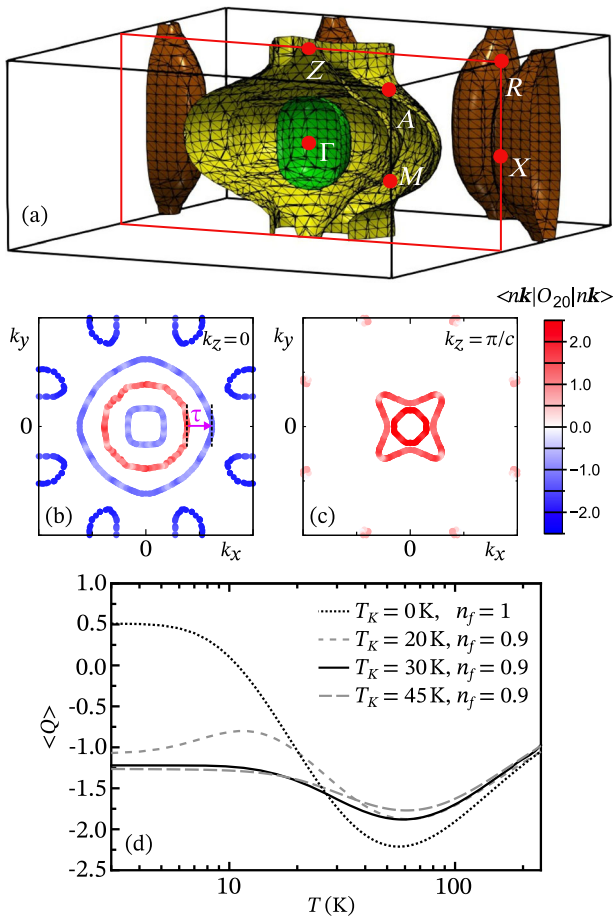


FIG. 5. Interplay of the Kondo effect and quadrupolar degrees of freedom for the low-energy excitations in  $\text{CeRh}_2\text{As}_2$ . In the figures,  $B_{44} > 0$  is chosen for the CEF scheme (see Supplemental Material [19]). Assuming  $B_{44} < 0$  leads to qualitatively similar results (see Supplemental Material [19]). (a) Quasiparticle FS as given by the RBS method for  $B_{44} > 0$ . Only half of the Brillouin zone is shown to reveal the FS structure. The characteristic features are two strongly corrugated cylinders (yellow) along  $\Gamma - Z$ , a  $\Gamma$ -centered closed surface (green), as well as corrugated cylinders (brown) along axes parallel to  $A - M$ . The yellow FS sheets belong to one band, and the green and brown FS sheets belong to another band. Several critical points in the vicinity of the Fermi energy  $E_F$  indicate the possibility of Lifshitz transitions. The sign of  $B_{44}$  affects the topology only weakly. (b),(c) Pronounced nesting features are seen from the intersections of the FS with the basal plane  $k_z = 0$  and the top plane  $k_z = \pi/c$ . The vector  $\tau$  indicates a possible nesting vector between the particlelike (red part) and the holelike (blue part) Fermi surfaces, which could be responsible for the formation of the QDW. The  $\mathbf{k}$ -dependent expectation values of  $\langle n\mathbf{k} | 3J_z^2 - \mathbf{J}^2 | n\mathbf{k} \rangle = \langle n\mathbf{k} | O_{20} | n\mathbf{k} \rangle$  highlight that quadrupolar degrees of freedom should play an important role in this material. (d) Variation with temperature of the quadrupole moment of the single-impurity Ce  $4f$  shell in the Kondo regime ( $T_K = 30$  K,  $n_f = 0.9$ , full line) differs both qualitatively and quantitatively from its counterpart in the local moment regime ( $T_K = 0$  K,  $n_f = 1$ , dotted line). We also include two curves (gray lines) for slightly different values of  $T_K$  to show that the results are similar, i.e., robust against small variation of  $T_K$ .

The calculations employ a simple approximation to the noncrossing approximation [42,43] for the Anderson model impurity Hamiltonian in the limit of large Coulomb repulsion  $U$ . The choice of the low-temperature  $4f$  valence in the Kondo regime  $n_f(T \rightarrow 0)$  enters mainly as an overall scale. In the low-temperature limit  $T \rightarrow 0$ , the Kondo effect strongly affects both the sign and the magnitude of  $Q(T \rightarrow 0)$ . We also include two curves for  $T_K = 20$  and  $45$  K, which correspond to the  $T_K$  limits set by the analysis of the entropy [8]: This shows that the change in  $\langle Q \rangle$  is not very sensitive to variation in  $T_K$  within this range. Thus, due to the strong mixing of the excited CEF doublets into the ground state, the quadrupole moment becomes a property which even at  $T = 0$  is very sensitive to change in the hybridization. That opens a door for quadrupolar or multipolar ordering.

The characteristic admixture of excited CEF states is also evident in the coherent heavy quasiparticles  $|n\mathbf{k}\rangle$  of band index  $n$  and wave number  $\mathbf{k}$  which form in a periodic Kondo lattice. The expectation values  $\langle n\mathbf{k} | 3J_z^2 - \mathbf{J}^2 | n\mathbf{k} \rangle$  in the states at the Fermi surface (FS) are strongly  $\mathbf{k}$  dependent as shown in Figs. 5(b) and 5(c). This demonstrates that quadrupolar degrees of freedom play an important role for the ground-state properties of  $\text{CeRh}_2\text{As}_2$ . Moreover, pronounced nesting features are seen from the intersections of the FS with the basal plane  $k_z = 0$  [Fig. 5(b)] and the top plane  $k_z = \pi/c$  [Fig. 5(c)]. So, if nesting occurs then the associated quadrupolar degrees of freedom will be affected. This property could link the observed opening of a gap in the plane at  $T_0$  with the transition observed in thermodynamic probes, as we discuss above.

The results of these theoretical calculations, i.e., the strong change in the quadrupole moment induced by the Kondo exchange, the large variation of the expectation value for the quadrupole moment across the Fermi surface, and the strong nesting properties of the Fermi surfaces, suggest a possible scenario which reconciles all observed properties: a quadrupolar or multipolar density wave (QDW) based on itinerant heavy  $4f$  electrons. This is a very unusual scenario. To the best of our knowledge, it has never been proposed before. It requires very specific properties of the  $4f$  electrons, which, however, are all fulfilled in the case of  $\text{CeRh}_2\text{As}_2$ : a significant strength of the Kondo interaction, an energy splitting to the first excited CEF doublet of the same size of the Kondo scale, a strong variability of the expectation of the quadrupole moment across the Fermi surface, and nesting features of the Fermi surface. Within this scenario, the unexpected and very unusual positive pressure dependence of  $T_0$  can easily be explained. Without doubt, pressure shall enhance the hybridization between  $4f$  and conduction electrons in  $\text{CeRh}_2\text{As}_2$  as it does in all known Ce-based HF systems, and is suggested by the positive Grüneisen parameter. That should increase the change in the quadrupole moment at  $T = 0$  as well as its sensitivity to hybridization, thus

promoting an itinerant QDW. On the other hand, the positive field dependence of  $T_0$  is likely due to the same mechanism as in standard, local quadrupolar ordered systems: There, the quadrupolar order is stabilized by a field-induced magnetic moment.

Another interesting example with a similar situation is YbSb [46,47]: A nonmagnetic transition at  $T_Q \approx 5$  K shows indications of quadrupolar order, although its CEF ground state is a Kramers doublet and the first excited state is at  $\Delta_1 \approx 170$  K. Attempts to explain this transition as a localized quadrupolar order induced by mixing of high excited CEF levels failed to reproduce the low ordering temperature and the weak field dependence because of the too large difference between  $\Delta_1$  and  $T_Q$  [48]. Since some features suggest that the hybridization between the  $4f$  and the conduction electrons is significant also in YbSb, the hybridization might be the key ingredient to understand its quadrupolar order as in CeRh<sub>2</sub>As<sub>2</sub>.

The antiferroquadrupolar phase (AFQ) in CeB<sub>6</sub> has been suggested to be driven by nesting as well [49,50], but there is a fundamental difference between the QDW state in CeRh<sub>2</sub>As<sub>2</sub> and the AFQ phase in CeB<sub>6</sub> (and similar systems). In CeB<sub>6</sub>—because of the cubic crystalline structure—the ground state has quadrupolar degrees of freedom without need of hybridization, whereas in CeRh<sub>2</sub>As<sub>2</sub> the Kramers doublet ground state has no quadrupolar degrees of freedom and acquires them only through hybridization. So, the QDW state in CeRh<sub>2</sub>As<sub>2</sub> is a purely itinerant effect, in contrast to the AFQ state in CeB<sub>6</sub> in which the quadrupolar moments can be considered as local. In CeB<sub>6</sub>, the hybridization is important in the sense that it enters the Ruderman-Kittel-Kasuya-Yosida interaction between the local quadrupoles [51] being therefore responsible for the choice of the ordering wave vector  $(\pi, \pi, \pi)$  of the AFQ phase due to strong nesting at this wave vector [49].

We might have in CeRh<sub>2</sub>As<sub>2</sub> an uncommon quadrupolar order of itinerant  $4f$  states induced by a strong  $4f$ -conduction electron hybridization which mixes excited CEF states into the ground state. In standard Ce- or Yb-based Kondo lattices, usually only the CEF ground state is relevant and taken into account for the properties at low  $T$ . In contrast, in this new itinerant QDW state the excited CEF levels are crucial. Thus, it presents some analogies to the recently proposed metaorbital scenario [20], in which at higher pressures a strongly correlated  $4f$  state is formed not out of the CEF ground state, but with the excited CEF state when the hybridization of this excited state is much stronger than that of the CEF ground state. We note that an unusual ordered state, with a very unusual phase diagram presenting some analogy to that of CeRh<sub>2</sub>As<sub>2</sub>, and where very likely excited CEF states are involved, has recently been observed in the tetragonal Kondo lattice CeCoSi [52]. As for CeRh<sub>2</sub>As<sub>2</sub>, the Ce site does not present inversion symmetry, while the overall structure is

centrosymmetric. At zero pressure, CeCoSi exhibits AFM order at 9 K, but under pressure, a new ordered state appears with an ordering temperature  $T^*$  shooting up to 38 K at a pressure of merely 1.2 GPa. Increasing pressure further to 2.2 GPa suppresses completely all ordered states, resulting in a strongly hybridized paramagnetic Kondo lattice. Recent NQR and NMR results proved that the state forming at  $T^*$  cannot be a dipolar order, instead a yet unidentified unusual kind of multipolar order was proposed [53]. However, inelastic neutron results and specific heat data put the first excited CEF doublet at 125 K above the ground-state doublet, making a standard quadrupolar order at 38 K impossible [54]. Therefore, a further interaction is required to stabilize multipolar order under such conditions. Since this unusual phase appears under pressure only slightly before the onset of the highly hybridized paramagnetic state, hybridization is expected to play an important role.

Concerning the nature of the high-field phase II in CeRh<sub>2</sub>As<sub>2</sub>, some insights can be gained from experimental observations: The large positive slope  $dT_0/dH$  precludes the main order parameter to be a dipolar AFM one. The absence of any anomaly in the ac susceptibility (Fig. S4 in Supplemental Material [19]) and the observation that the signature of the transition becomes sharper with increasing field exclude a dipolar FM order parameter. The large positive slope  $dT_0/dH$  and the vertical first-order phase boundary at  $\mu_0 H_{cr} = 9$  T with a large anomaly in the magnetostriction are reminiscent of observation in quadrupolar ordered systems like, for example, Ce<sub>3</sub>Pd<sub>20</sub>Si<sub>6</sub> [55]. In these systems, the field-induced magnetic moment couples to multipolar degrees of freedom, inducing new multipolar states which are stabilized by an increasing magnetic field (see, e.g., Ref. [56] about PrPb<sub>3</sub>). Similar experimental features have been observed, e.g., in Ce<sub>0.5</sub>La<sub>0.5</sub>B<sub>6</sub>: In this compound, the crossover to phase IV is characterized by a large maximum in  $C/T$  in zero field (similar to what we see at  $T_0$  in CeRh<sub>2</sub>As<sub>2</sub>), and a magnetic field  $H \parallel [110]$  induces a very sharp phase transition from the AF octupolar (phase IV) into the AF quadrupolar phase (phase II) [38]. As in CeRh<sub>2</sub>As<sub>2</sub>, the transition temperature in the high-field phase increases steeply with increasing field, and all magnetic features observed at the critical field are weak. This strong similarity obviously suggests that the transition at  $\mu_0 H_{cr} = 9$  T in CeRh<sub>2</sub>As<sub>2</sub> marks the change to a different multipolar order parameter stabilized by the field-induced magnetic moment. In contrast to the situation in CeB<sub>6</sub>, in CeRh<sub>2</sub>As<sub>2</sub> the ordering multipolar degree of freedom must be a highly itinerant  $4f$  one.

### III. CONCLUSION

To conclude, the present study confirms that the superconducting state in the locally noncentrosymmetric Kondo lattice CeRh<sub>2</sub>As<sub>2</sub> is preceded by an ordered state, phase I, with a transition temperature  $T_0 = 0.4$  K above

$T_c = 0.26$  K. Phase I changes into a second phase II through a first-order phase transition at an in-plane magnetic field of 9 T. Both phases present unusual features which are incompatible with the usually expected dipolar magnetic order. Instead, all experimental results, as well as RBS calculations, point to a unique case of quadrupole-density-wave order in phases I and II. This is made possible in  $\text{CeRh}_2\text{As}_2$  by a comparatively large  $T_K$  and a small crystal field splitting, which results in a very strong mixing of excited CEF doublets into the ground-state doublet. As a result, the heavy bands acquire quadrupolar degrees of freedom, which together with strong nesting properties open the way for quadrupolar density waves. The Pauli-limited superconducting phase SC1 is entirely included within phase I (see Fig. 4). If the order parameter of phase I was originating from completely localized  $4f$  states, then one would expect coexistence of SC and phase I with only limited interference, as, e.g., in the rare-earth borocarbides [57]. But there is no doubt that the  $4f$  electrons are strongly delocalized in phases I and II of  $\text{CeRh}_2\text{As}_2$ . Then one would expect a strong interference between SC and phase I if, e.g., the SC gap and the gap of phase I opens on the same sheet of the Fermi surface. However, right now there is no clear experimental evidence of how the SC state and phase I are interacting.

#### ACKNOWLEDGMENTS

We are indebted to D. Agterberg, H.-U. Desgranges, D. Inosov, K. Ishida, A. P. Mackenzie, H. Rosner, O. Stockert and P. Thalmeier for useful discussions. We would like to thank the Deutsche Forschungsgemeinschaft (DFG) Projects No. BR 4110/1-1 and No. KU 3287/1-1 for financial support. This work is also supported by the joint Agence National de la Recherche and DFG program Fermi-NESr through Grants No. GE602/4-1 (C. G.) and No. ZW77/5-1 (G. Z.).

- 
- [1] F. Steglich, J. Aarts, C. D. Bredl, W. Lieke, D. Meschede, W. Franz, and H. Schäfer, *Superconductivity in the Presence of Strong Pauli Paramagnetism: CeCu<sub>2</sub>Si<sub>2</sub>*, *Phys. Rev. Lett.* **43**, 1892 (1979).
- [2] R. A. Fisher, S. Kim, B. F. Woodfield, N. E. Phillips, L. Taillefer, K. Hasselbach, J. Flouquet, A. L. Giorgi, and J. L. Smith, *Specific Heat of UPt<sub>3</sub>: Evidence for Unconventional Superconductivity*, *Phys. Rev. Lett.* **62**, 1411 (1989).
- [3] G. Bruls, D. Weber, B. Wolf, P. Thalmeier, B. Lüthi, A. d. Visser, and A. Menovsky, *Strain–Order-Parameter Coupling and Phase Diagrams in Superconducting UPt<sub>3</sub>*, *Phys. Rev. Lett.* **65**, 2294 (1990).
- [4] S. Adenwalla, S. W. Lin, Q. Z. Ran, Z. Zhao, J. B. Ketterson, J. A. Sauls, L. Taillefer, D. G. Hinks, M. Levy, and B. K. Sarma, *Phase Diagram of UPt<sub>3</sub> from Ultrasonic Velocity Measurements*, *Phys. Rev. Lett.* **65**, 2298 (1990).
- [5] J. A. Sauls, *The Order Parameter for the Superconducting Phases of UPt<sub>3</sub>*, *Adv. Phys.* **43**, 113 (1994).
- [6] R. Joynt and L. Taillefer, *The Superconducting Phases of UPt<sub>3</sub>*, *Rev. Mod. Phys.* **74**, 235 (2002).
- [7] T. Yoshida, M. Sigrist, and Y. Yanase, *Pair-Density Wave States through Spin-Orbit Coupling in Multilayer Superconductors*, *Phys. Rev. B* **86**, 134514 (2012).
- [8] S. Khim, J. F. Landaeta, J. Banda, N. Bannor, M. Brando, P. M. R. Brydon, D. Hafner, R. KÜchler, R. Cardoso-Gil, U. Stockert *et al.*, *Field-Induced Transition within the Superconducting State of CeRh<sub>2</sub>As<sub>2</sub>*, *Science* **373**, 1012 (2021).
- [9] P. Monthoux, D. Pines, and G. G. Lonzarich, *Superconductivity without Phonons*, *Nature (London)* **450**, 1177 (2007).
- [10] M. Kibune, S. Kitagawa, K. Kinjo, S. Ogata, M. Manago, T. Taniguchi, K. Ishida, M. Brando, E. Hassinger, H. Rosner, C. Geibel, and S. Khim, companion Letter, *Observation of Antiferromagnetic Order as Odd-Parity Multipoles inside the Superconducting Phase in CeRh<sub>2</sub>As<sub>2</sub>*, *Phys. Rev. Lett.* **128**, 057002 (2022).
- [11] G. Zwicknagl, *Quasi-Particles in Heavy Fermion Systems*, *Adv. Phys.* **41**, 203 (1992).
- [12] G. Zwicknagl, *Quasiparticles in Heavy Fermion Systems*, *Phys. Scr.* **T49A**, 34 (1993).
- [13] G. Zwicknagl, *Field-Induced Suppression of the Heavy-Fermion State in YbRh<sub>2</sub>Si<sub>2</sub>*, *J. Phys. Condens. Matter* **23**, 094215 (2011).
- [14] G. Zwicknagl, *The Utility of Band Theory in Strongly Correlated Electron Systems*, *Rep. Prog. Phys.* **79**, 124501 (2016).
- [15] N. E. Christensen, *Relativistic Band Structure Calculations*, *Int. J. Quantum Chem.* **25**, 233 (1984).
- [16] G. Zwicknagl, E. Runge, and N. Christensen, *Low-Energy Excitations in Heavy Fermion Systems*, *Physica (Amsterdam)* **163B**, 97 (1990).
- [17] O. Stockert, E. Faulhaber, G. Zwicknagl, N. Stüßler, H. S. Jeevan, M. Deppe, R. Borth, R. KÜchler, M. Loewenhaupt, C. Geibel *et al.*, *Nature of the A Phase in CeCu<sub>2</sub>Si<sub>2</sub>*, *Phys. Rev. Lett.* **92**, 136401 (2004).
- [18] H. Pfau, R. Daou, S. Lausberg, H. R. Naren, M. Brando, S. Friedemann, S. Wirth, T. Westerkamp, U. Stockert, P. Gegenwart *et al.*, *Interplay between Kondo Suppression and Lifshitz Transitions in YbRh<sub>2</sub>Si<sub>2</sub> at High Magnetic Fields*, *Phys. Rev. Lett.* **110**, 256403 (2013).
- [19] See Supplemental Material at <http://link.aps.org/supplemental/10.1103/PhysRevX.12.011023> for information about the samples and additional measurements. It also includes a detailed analysis of the CEF scheme of  $\text{CeRh}_2\text{As}_2$ .
- [20] K. Hattori, *Meta-Orbital Transition in Heavy-Fermion Systems: Analysis by Dynamical Mean Field Theory and Self-Consistent Renormalization Theory of Orbital Fluctuations*, *J. Phys. Soc. Jpn.* **79**, 114717 (2010).
- [21] A. de Visser, J. Franse, A. Lacerda, P. Haen, and J. Flouquet, *Grüneisen Parameters of Heavy Fermion Systems*, *Physica (Amsterdam)* **163B**, 49 (1990).
- [22] S. Doniach, *Valence Instability and Related Narrow Band Phenomena* (Plenum, New York, 1977).
- [23] A. L. Cornelius, J. S. Schilling, D. Mandrus, and J. D. Thompson, *Anomalous Hydrostatic Pressure Dependence*



- of the Curie Temperature of the Kondo-Lattice compound  $\text{YbNiSn}$  to 38 GPa, *Phys. Rev. B* **52**, R15699 (1995).
- [24] N. Oeschler, P. Gegenwart, M. Lang, R. Movshovich, J. L. Sarrao, J. D. Thompson, and F. Steglich, *Uniaxial Pressure Effects on  $\text{CeIrIn}_5$  and  $\text{CeCoIn}_5$  Studied by Low-Temperature Thermal Expansion*, *Phys. Rev. Lett.* **91**, 076402 (2003).
- [25] L. Zhu, M. Garst, A. Rosch, and Q. Si, *Universally Diverging Grüneisen Parameter and the Magnetocaloric Effect Close to Quantum Critical Points*, *Phys. Rev. Lett.* **91**, 066404 (2003).
- [26] R. KÜchler, N. Oeschler, P. Gegenwart, T. Cichorek, K. Neumaier, O. Tegus, C. Geibel, J. A. Mydosh, F. Steglich, L. Zhu *et al.*, *Divergence of the Grüneisen Ratio at Quantum Critical Points in Heavy Fermion Metals*, *Phys. Rev. Lett.* **91**, 066405 (2003).
- [27] A. Steppke, R. KÜchler, S. Lausberg, E. Lengyel, L. Steinke, R. Borth, T. Lühmann, C. Krellner, M. Nicklas, C. Geibel *et al.*, *Ferromagnetic Quantum Critical Point in the Heavy-Fermion Metal  $\text{YbNi}_4(\text{P}_{1-x}\text{As}_x)_2$* , *Science* **339**, 933 (2013).
- [28] S. Watanabe and K. Miyake, *Grüneisen Parameter and Thermal Expansion near Magnetic Quantum Critical Points in Itinerant Electron Systems*, *Phys. Rev. B* **99**, 035108 (2019).
- [29] E. Hassinger, G. Knebel, K. Izawa, P. Lejay, B. Salce, and J. Flouquet, *Temperature-Pressure Phase Diagram of  $\text{URu}_2\text{Si}_2$  from Resistivity Measurements and *ac* Calorimetry: Hidden Order and Fermi-Surface Nesting*, *Phys. Rev. B* **77**, 115117 (2008).
- [30] M. D. Bachmann, G. M. Ferguson, F. Theuss, T. Meng, C. Putzke, T. Helm, K. R. Shirer, Y.-S. Li, K. A. Modic, M. Nicklas *et al.*, *Spatial Control of Heavy-Fermion Superconductivity in  $\text{CeIrIn}_5$* , *Science* **366**, 221 (2019).
- [31] S. Hamann, J. Zhang, D. Jang, A. Hannaske, L. Steinke, S. Lausberg, L. Pedrero, C. Klingner, M. Baenitz, F. Steglich *et al.*, *Evolution from Ferromagnetism to Antiferromagnetism in  $\text{Yb}(\text{Rh}_{1-x}\text{Co}_x)_2\text{Si}_2$* , *Phys. Rev. Lett.* **122**, 077202 (2019).
- [32] T. Gruner, D. Jang, Z. Huesges, R. Cardoso-Gil, G. H. Fecher, M. M. Koza, O. Stockert, A. Mackenzie, M. Brando, and C. Geibel, *Charge Density Wave Quantum Critical Point with Strong Enhancement of Superconductivity*, *Nat. Phys.* **13**, 967 (2017).
- [33] H. Pfau, R. Daou, S. Friedemann, S. Karbassi, S. Ghannadzadeh, R. KÜchler, S. Hamann, A. Steppke, D. Sun, M. König *et al.*, *Cascade of Magnetic-Field-Induced Lifshitz Transitions in the Ferromagnetic Kondo Lattice Material  $\text{YbNi}_4\text{P}_2$* , *Phys. Rev. Lett.* **119**, 126402 (2017).
- [34] F. Weickert, M. Brando, F. Steglich, P. Gegenwart, and M. Garst, *Universal Signatures of the Metamagnetic Quantum Critical Endpoint: Application to  $\text{CeRu}_2\text{Si}_2$* , *Phys. Rev. B* **81**, 134438 (2010).
- [35] M. Deppe, S. Lausberg, F. Weickert, M. Brando, Y. Skourski, N. Caroca-Canales, C. Geibel, and F. Steglich, *Pronounced First-Order Metamagnetic Transition in the Paramagnetic Heavy-Fermion System  $\text{CeTiGe}$* , *Phys. Rev. B* **85**, 060401(R) (2012).
- [36] J. Effantin, J. Rossat-Mignod, P. Burlet, H. Bartholin, S. Kunii, and T. Kasuya, *Magnetic Phase Diagram of  $\text{CeB}_6$* , *J. Magn. Magn. Mater.* **47–48**, 145 (1985).
- [37] A. S. Cameron, G. Friemel, and D. S. Inosov, *Multipolar Phases and Magnetically Hidden Order: Review of the Heavy-Fermion Compound  $\text{Ce}_{1-x}\text{La}_x\text{B}_6$* , *Rep. Prog. Phys.* **79**, 066502 (2016).
- [38] D. Jang, P. Y. Portnichenko, A. S. Cameron, G. Friemel, A. V. Dukhnenko, N. Y. Shitsevalova, V. B. Filipov, A. Schneidewind, A. Ivanov, D. S. Inosov *et al.*, *Large Positive Correlation between the Effective Electron Mass and the Multipolar Fluctuation in the Heavy-Fermion Metal  $\text{Ce}_{1-x}\text{La}_x\text{B}_6$* , *npj Quantum Mater.* **2**, 62 (2017).
- [39] J. Kitagawa, N. Takeda, and M. Ishikawa, *Possible Quadrupolar Ordering in a Kondo-Lattice Compound  $\text{Ce}_3\text{Pd}_{20}\text{Ge}_6$* , *Phys. Rev. B* **53**, 5101 (1996).
- [40] H. S. Jeevan, C. Geibel, and Z. Hossain, *Quasiquartet Crystal-Electric-Field Ground State with Possible Quadrupolar Ordering in the Tetragonal Compound  $\text{YbRu}_2\text{Ge}_2$* , *Phys. Rev. B* **73**, 020407(R) (2006).
- [41] T. Takimoto and P. Thalmeier, *Theory of Induced Quadrupolar Order in Tetragonal  $\text{YbRu}_2\text{Ge}_2$* , *Phys. Rev. B* **77**, 045105 (2008).
- [42] V. Zevin, G. Zwickyagl, and P. Fulde, *Temperature Dependence of the 4f Quadrupole Moment of Yb in  $\text{YbCu}_2\text{Si}_2$* , *Phys. Rev. Lett.* **60**, 2331 (1988).
- [43] G. Zwickyagl, V. Zevin, and P. Fulde, *Simple Approximation Scheme for the Anderson Impurity Hamiltonian*, *Z. Phys. B* **79**, 365 (1990).
- [44] T. Yamada and K. Hanzawa, *Derivation of RKKY Interaction between Multipole Moments in  $\text{CeB}_6$  by the Effective Wannier Model Based on the Bandstructure Calculation*, *J. Phys. Soc. Jpn.* **88**, 084703 (2019).
- [45] R. Tazai and H. Kontani, *Multipole Fluctuation Theory for Heavy Fermion Systems: Application to Multipole Orders in  $\text{CeB}_6$* , *Phys. Rev. B* **100**, 241103(R) (2019).
- [46] K. Hashi, H. Kitazawa, A. Oyamada, and H. A. Katori, *Mixing-Typed Antiferroquadrupolar Ordering in  $\text{YbSb}$* , *J. Phys. Soc. Jpn.* **70**, 259 (2001).
- [47] A. Yamamoto, J. Takeda, T. Koyama, T. Mito, S. Wada, I. Shirovani, and C. Sekine, *Evidence for an Antiferroquadrupolar Ordering in  $\text{YbSb}$  Probed by *Sb* 121 and *Sb* 123 Nuclear Magnetic Resonances*, *Phys. Rev. B* **70**, 220402(R) (2004).
- [48] A. Oyamada, S. Maegawa, T. Goto, K. Hashi, and H. Kitazawa, *Quadrupolar Ordering in  $\text{YbSb}$  Studied by  $^{121}\text{Sb}$  and  $^{123}\text{Sb}$  NMR*, *J. Phys. Soc. Jpn.* **73**, 1953 (2004).
- [49] A. Koitzsch, N. Heming, M. Knupfer, B. Büchner, P. Y. Portnichenko, A. V. Dukhnenko, N. Y. Shitsevalova, V. B. Filipov, L. L. Lev, V. N. Strocov *et al.*, *Nesting-Driven Multipolar Order in  $\text{CeB}_6$  from Photoemission Tomography*, *Nat. Commun.* **7**, 10876 (2016).
- [50] S. E. Nikitin, P. Y. Portnichenko, A. V. Dukhnenko, N. Y. Shitsevalova, V. B. Filipov, Y. Qiu, J. A. Rodriguez-Rivera, J. Ollivier, and D. S. Inosov, *Doping-Induced Redistribution of Magnetic Spectral Weight in the Substituted Hexaborides  $\text{Ce}_{1-x}\text{La}_x\text{B}_6$  and  $\text{Ce}_{1-x}\text{Nd}_x\text{B}_6$* , *Phys. Rev. B* **97**, 075116 (2018).
- [51] H. Shiba, O. Sakai, and R. Shiina, *Nature of Ce-Ce Interaction in  $\text{CeB}_6$  and Its Consequences*, *J. Phys. Soc. Jpn.* **68**, 1988 (1999).

- [52] E. Lengyel, M. Nicklas, N. Caroca-Canales, and C. Geibel, *Temperature-Pressure Phase Diagram of CeCoSi: Pressure-Induced High-Temperature Phase*, *Phys. Rev. B* **88**, 155137 (2013).
- [53] M. Manago, H. Kotegawa, H. Tou, H. Harima, and H. Tanida, *Unusual Nonmagnetic Ordered State in CeCoSi Revealed by  $^{59}\text{Co}$ -NMR and NQR Measurements*, *J. Phys. Soc. Jpn.* **90**, 023702 (2021).
- [54] S. E. Nikitin, D. G. Franco, J. Kwon, R. Bewley, A. Podlesnyak, A. Hoser, M. M. Koza, C. Geibel, and O. Stockert, *Gradual Pressure-Induced Enhancement of Magnon Excitations in CeCoSi*, *Phys. Rev. B* **101**, 214426 (2020).
- [55] P. Y. Portnichenko, S. Paschen, A. Prokofiev, M. Vojta, A. S. Cameron, J.-M. Mignot, A. Ivanov, and D. S. Inosov, *Incommensurate Short-Range Multipolar Order Parameter of Phase II in  $\text{Ce}_3\text{Pd}_{20}\text{Si}_6$* , *Phys. Rev. B* **94**, 245132 (2016).
- [56] T. Onimaru, T. Sakakibara, N. Aso, H. Yoshizawa, H. S. Suzuki, and T. Takeuchi, *Observation of Modulated Quadrupolar Structures in  $\text{PrPb}_3$* , *Phys. Rev. Lett.* **94**, 197201 (2005).
- [57] N. H. Andersen, J. Jensen, T. B. S. Jensen, M. v. Zimmermann, R. Pinholt, A. B. Abrahamsen, K. N. Toft, P. Hedegård, and P. C. Canfield, *Phonon-Induced Quadrupolar Ordering of the Magnetic Superconductor  $\text{TmNi}_2\text{B}_2\text{C}$* , *Phys. Rev. B* **73**, 020504(R) (2006).